

# Single vibronic level fluorescence spectra from Hagedorn wavepacket dynamics

Zhan Tong Zhang and Jiří J. L. Vaníček<sup>a)</sup>

Laboratory of Theoretical Physical Chemistry, Institut des Sciences et Ingénierie Chimiques, Ecole Polytechnique Fédérale de Lausanne (EPFL), CH-1015 Lausanne, Switzerland

(Dated: 17 December 2024)

In single vibronic level (SVL) fluorescence experiments, the electronically excited initial state is also excited in one or several vibrational modes. Because computing such spectra by evaluating all contributing Franck-Condon factors becomes impractical (and unnecessary) in large systems, here we propose a time-dependent approach based on Hagedorn wavepacket dynamics. We use Hagedorn functions—products of a Gaussian and carefully generated polynomials—to represent SVL initial states because in systems whose potential is at most quadratic, Hagedorn functions are exact solutions to the time-dependent Schrödinger equation and can be propagated with the same equations of motion as a simple Gaussian wavepacket. Having developed an efficient recursive algorithm to compute the overlaps between two Hagedorn wavepackets, we can now evaluate emission spectra from arbitrary vibronic levels using a single trajectory. We validate the method in two-dimensional global harmonic models by comparing it with quantum split-operator calculations. Additionally, we study the effects of displacement, distortion (squeezing), and Duschinsky rotation on SVL fluorescence spectra. Finally, we demonstrate the applicability of the Hagedorn approach to high-dimensional systems on a displaced, distorted, and Duschinsky-rotated harmonic model with 100 degrees of freedom.

## I. INTRODUCTION

Vibronic spectroscopy offers valuable insights into the quantum dynamics of molecules.<sup>1</sup> In single vibronic level (SVL) fluorescence spectroscopy, tuned narrow-band lasers are used to prepare a population of molecules excited to a specific vibronic level. Measuring the subsequent fluorescence decay of such a system can provide important information about vibrational structures, excited-state relaxation, as well as the vibronic coupling between ground and excited states.<sup>2–8</sup>

The simulation of SVL spectra of small molecules has been carried out using time-independent sum-over-states expressions,<sup>9–15</sup> but the computation of Franck-Condon factors in larger molecules becomes more challenging with the increasing number of vibrational states involved, especially due to the non-separable overlap integrals under Duschinsky mixing effects. Methods based on the time-dependent picture are more efficient for larger systems and constitute a more fundamental approach that is naturally suited to simulating time-resolved and multidimensional spectroscopy.<sup>16–20</sup> Like the time-independent approach, the time-dependent one can also readily incorporate Duschinsky rotation, Herzberg-Teller,<sup>21–26</sup> and temperature effects.<sup>27–30</sup> Although the time-dependent approach has been applied to SVL<sup>31,32</sup> and similar experiments,<sup>33–35</sup> its practical application has been confined to initial states excited at most to the first excited vibrational level and only in a single vibrational mode.

In the case of absorption or emission from the ground vibrational state, the thawed Gaussian approximation<sup>36–38</sup> (TGA) has been successful in

simulating vibrationally resolved electronic spectra in situations where a single Gaussian represents the evolving wavefunction reasonably well.<sup>18,28,29,39–43</sup> However, the SVL emission process involving a vibrationally excited initial state cannot be described by a single Gaussian wavepacket even at the initial time. Within the harmonic approximation, it may instead be captured, at all times, by a Gaussian multiplied by a polynomial. Tapavicza’s efficient generating function approach<sup>32</sup> can treat initial states singly excited in one mode, whereas the extended TGA<sup>22,25,28,44–46</sup> (ETGA) may accommodate simultaneous single excitations in multiple modes, but only in systems without Duschinsky rotation.<sup>47</sup> A more general method is needed for situations where the simultaneous excitation of *multiple* vibrational modes to *higher* levels is involved.

By generalizing Dirac’s ladder operators for one-dimensional quantum harmonic oscillators to arbitrary dimensions, Hagedorn introduced a special pair of raising and lowering operators that generate a series of functions in the form of a Gaussian wavepacket multiplied by a polynomial.<sup>48–53</sup> Unlike simple products of one-dimensional Hermite functions, Hagedorn functions are exact solutions to the time-dependent Schrödinger equation (TDSE) with an arbitrary many-dimensional harmonic potential when the parameters of the associated Gaussian are propagated with classical-like equations of motion. Hagedorn functions also form a complete orthonormal basis that may be used to expand arbitrary numerically exact solutions to the TDSE with a general potential.<sup>54</sup> However, in this work, we consider exclusively Hagedorn wavepackets consisting of only one Hagedorn function at all times. Henceforth, we use “Hagedorn wavepackets” and “Hagedorn functions” synonymously.

Despite their promising properties<sup>52,53,55–57</sup> and a few applications in quantum and chemical physics,<sup>54,58–66</sup>

<sup>a)</sup>Electronic mail: jiri.vanicek@epfl.ch

Hagedorn wavepackets have yet to be applied to spectroscopic simulation, since one important ingredient, an efficient way to compute the correlation functions between two Hagedorn wavepackets, was missing. Having developed an efficient algebraic algorithm for this overlap in Ref. 67, we can now apply the Hagedorn approach to the simulation of SVL spectra.

Here, we first use the Hagedorn wavepacket dynamics to compute SVL emissions from different vibrational levels in two-dimensional harmonic models, where we can validate the results with “exact” quantum split-operator calculations. We also examine how nuclear displacement, mode distortion (squeezing), and Duschinsky rotation (mode mixing) influence SVL spectra by analyzing the different spectra arising from three harmonic models that gradually incorporate these effects. One important advantage of our approach is that the propagation of Hagedorn wavepackets does not incur any additional computational cost in harmonic potentials beyond that of propagating a single Gaussian wavepacket. The Hagedorn approach is thus suitable for much higher dimensions than grid-based quantum methods, and we demonstrate this by computing spectra of a two-state harmonic model system with 100 vibrational degrees of freedom.

## II. THEORY

Let  $|K\rangle \equiv |e, K\rangle$  denote a specific vibrational state on the adiabatic potential energy surface of the excited electronic state  $e$ , where  $K = (K_1, \dots, K_D)$  is the multi-index of non-negative integers specifying the vibrational quantum numbers in the  $D$  normal modes. Within the Condon approximation, the emission rate from  $|K\rangle$  to the ground electronic state  $g$  may be obtained by the Fourier transform<sup>32,68</sup>

$$\sigma_{\text{em}}(\omega) = \frac{4\omega^3}{3\pi\hbar c^3} |\mu_{ge}|^2 \text{Re} \int_0^\infty \overline{C(t)} \exp[it(\omega - E_{e,K}/\hbar)] dt \quad (1)$$

of the wavepacket autocorrelation function

$$C(t) = \langle K | \exp(-i\hat{H}_g t/\hbar) | K \rangle. \quad (2)$$

Here,  $\mu_{ge}$  is the electronic transition dipole moment,  $\hat{H}_g$  is the nuclear Hamiltonian associated with the ground electronic state,  $E_{e,K} = \hbar\omega_{e,K}$  is the total electronic and vibrational energy of the initial state, and the bar [e.g., in  $\overline{C(t)}$ ] indicates the complex conjugate (we avoid using  $*$  to prevent confusion with its use for the conjugate transpose in the mathematical literature on Hagedorn wavepackets). In this time-dependent framework, the initial wavepacket is evolved on the ground-state surface, and the overlaps between the initial wavepacket  $|K\rangle$  and the propagated wavepacket  $e^{-i\hat{H}_g t/\hbar}|K\rangle$  are computed in order to evaluate the spectrum.

Solving the time-dependent Schrödinger equation is a challenging numerical problem. Hagedorn’s semiclassical wavepackets offer a practical approach to evolve

a wavepacket in higher-dimensional systems.<sup>48,51,53</sup> In Hagedorn’s parametrization,<sup>53,54,69</sup> a normalized  $D$ -dimensional Gaussian wavepacket is written as

$$\varphi_0[\Lambda_t, S_t](q) = \frac{1}{(\pi\hbar)^{D/4} \sqrt{\det(Q_t)}} \times \exp \left[ \frac{i}{\hbar} \left( \frac{1}{2} x^T \cdot P_t \cdot Q_t^{-1} \cdot x + p_t^T \cdot x + S_t \right) \right], \quad (3)$$

with the shifted position  $x := q - q_t$ , a phase term  $S_t$  related to the classical action, and a set of time-dependent parameters  $\Lambda_t = (q_t, p_t, Q_t, P_t)$ , where  $q_t$  and  $p_t$  represent the position and momentum of the wavepacket’s center, and  $Q_t$  and  $P_t$  are complex-valued  $D$ -dimensional matrices related by<sup>69</sup>

$$\text{Cov}(\hat{q}) = (\hbar/2)Q_t \cdot Q_t^\dagger, \quad \text{Cov}(\hat{p}) = (\hbar/2)P_t \cdot P_t^\dagger \quad (4)$$

to the position and momentum covariances. The two matrices replace the “width matrix”  $A_t = P_t \cdot Q_t^{-1}$  used in Heller’s parametrization<sup>53,69,70</sup> and satisfy the symplecticity conditions<sup>52,53</sup>

$$Q_t^T \cdot P_t - P_t^T \cdot Q_t = 0, \quad (5)$$

$$Q_t^\dagger \cdot P_t - P_t^\dagger \cdot Q_t = 2i\text{Id}, \quad (6)$$

where Id is the  $D$ -dimensional identity matrix.

Hagedorn defined a special pair of raising and lowering operators,<sup>51,53</sup>

$$A^\dagger \equiv A^\dagger[\Lambda_t] := \frac{i}{\sqrt{2\hbar}} \left( P_t^\dagger \cdot \hat{x} - Q_t^\dagger \cdot \hat{y} \right), \quad (7)$$

$$A \equiv A[\Lambda_t] := -\frac{i}{\sqrt{2\hbar}} \left( P_t^T \cdot \hat{x} - Q_t^T \cdot \hat{y} \right), \quad (8)$$

where  $\hat{x} := \hat{q} - q_t$  and  $\hat{y} := \hat{p} - p_t$  are the shifted position and momentum operators. The ladder operators connect the thawed Gaussian wavepacket  $\varphi_0$  to a family of Hagedorn functions  $\varphi_K$  in the form of a Gaussian multiplied by a polynomial, such that

$$\varphi_{K+(j)} = \frac{1}{\sqrt{K_j + 1}} A_j^\dagger \varphi_K, \quad (9)$$

$$\varphi_{K-(j)} = \frac{1}{\sqrt{K_j}} A_j \varphi_K, \quad (10)$$

where  $\langle j \rangle = (\underbrace{0, \dots, 0}_{j-1}, 1, \underbrace{0, \dots, 0}_{D-j})$  is the  $D$ -dimensional

unit vector with components  $\langle j \rangle_k \equiv \delta_{jk}$ .<sup>48,51–53</sup> In Eqs. (9) and (10), the  $j$ -th components of  $A^\dagger$  and  $A$  respectively raise and lower the  $j$ -th component of the multi-index  $K$  of the Hagedorn function  $\varphi_K$  by a unity. In general, the polynomial factor cannot be expressed as a product of univariate polynomials.<sup>50,53,71,72</sup>

However, in the special case where the inverse of  $Q_t$  times the complex conjugate of  $Q_t$  results in a diagonal  $Q_t^{-1} \cdot \overline{Q_t}$  matrix, the polynomial factor of a Hagedorn

function can be represented as a product of scaled Hermite polynomials  $H_n$ .<sup>53</sup> If we adopt the mass-weighted normal-mode coordinates of the excited-state potential energy surface, the “position” matrix  $Q_0$  of the initial state may be chosen to be diagonal with  $Q_{0,jj} = (m_j \omega_j)^{-1/2}$ , where  $\omega_j$  is the angular frequency of the  $j$ -th vibrational mode with a common mass  $m_j = m$ . In this case, the initial Hagedorn function

$$\varphi_K(q) = \langle q|K\rangle = \frac{\varphi_0(q)}{\sqrt{2^{|K|} K!}} \prod_{j=1}^D H_{K_j} \left( \sqrt{\frac{m\omega_j}{\hbar}} \cdot x_j \right) \quad (11)$$

is exactly the vibrational eigenfunction of a harmonic Hamiltonian and can thus represent the SVL initial state.

Notably, Hagedorn wavepackets, like thawed Gaussians, are exact solutions to the time-dependent Schrödinger equation in a harmonic potential

$$V(q) = v_0 + (q - q_{\text{ref}})^T \cdot \kappa \cdot (q - q_{\text{ref}})/2, \quad (12)$$

which generally serves as a good approximation of the molecular potential energy surface near the equilibrium nuclear configuration. The parameters of the Gaussian associated with the Hagedorn wavepacket evolve according to the equations

$$\dot{q}_t = m^{-1} \cdot p_t, \quad (13)$$

$$\dot{p}_t = -V'(q_t) \quad (14)$$

$$\dot{Q}_t = m^{-1} \cdot P_t, \quad (15)$$

$$\dot{P}_t = -V''(q_t) \cdot Q_t, \quad (16)$$

$$\dot{S}_t = L_t, \quad (17)$$

which are the same as the equations for propagating a purely Gaussian wavepacket.<sup>51,53,69</sup> Here, the subscript  $t$  denotes the time,  $m$  the real symmetric mass matrix (scalar in mass-weighted normal-mode coordinates), and  $L_t$  is the Lagrangian.

To finally obtain SVL spectra from the dynamics results, the evaluation of overlap integrals (2) between two Hagedorn wavepackets with different Gaussian parameters is needed. However, a straightforward analytical expression, like that available for overlaps between two Gaussian wavepackets, has remained elusive for Hagedorn wavepackets. Past applications of Hagedorn wavepackets require numerical quadrature for integrals, which becomes challenging in higher dimensions.<sup>54,60,62–66</sup> In Ref. 67, we have instead proposed a recursive algebraic scheme to compute these overlaps. This allows us to apply Hagedorn wavepackets in much higher dimensions, paving the way for their spectroscopic applications.

Remarkably, Hagedorn wavepackets enable the evaluation of SVL emission spectra from *any* vibrational level using a single trajectory  $(\Lambda_t, S_t)$  of the common guiding Gaussian. Therefore, regardless of the initial excitation, the electronic structure calculations (computationally much more expensive than the overlaps) need to be performed only once in real molecular applications.

Hagedorn wavepackets can be seen as a generalization of coherent states,<sup>51,55,72–74</sup> and our approach is thus connected to the generating function formalism proposed by Huh and Berger.<sup>31</sup> Although their expressions, relying on multivariate Hermite polynomials, are also general for arbitrary initial vibrational levels, no implementation or application was given. As far as we know, the only practical formulation is that of Tapavicza,<sup>32</sup> which is so far limited to single excitation in one mode. The Hagedorn approach, in addition to its generality, also provides a more intuitive time-dependent picture and offers a straightforward propagation scheme.

In this study, we focus solely on global harmonic models so that the results can be analyzed without additional approximation or errors. Whereas anharmonicity<sup>24,75–77</sup> and non-adiabatic<sup>78</sup> effects must be taken into account in many situations, adiabatic harmonic potentials have served as a useful starting point for computing and assigning the spectra of many molecules.<sup>9,32,34,35,79–86</sup>

### III. NUMERICAL EXAMPLES

#### A. Two-dimensional harmonic potentials

We begin by considering two-dimensional model systems. They are the simplest multi-dimensional cases where, in the presence of Duschinsky rotation (mode mixing), the dynamics of Hagedorn wavepackets differ from that of simple products of one-dimensional Hermite functions. Additionally, numerically exact quantum calculations are readily accessible for the verification of the surprisingly complicated spectra of these models.

We assume that the initial, excited-state electronic surface  $V_e$  and the final, ground-state electronic surface  $V_g$  can both be described by a quadratic function (12). In all cases, the ground-state surface  $V_g$  is centered at  $q_{\text{ref},g} = (0, 0)$ , and the initial wavepacket is centered at  $q_0 = q_{\text{ref},e} = (15, -15)$ , i.e., at the minimum of the excited-state surface  $V_e$ , and has zero momentum  $p_0 = (0, 0)$ . The positions, provided in atomic units, are in the mass-weighted excited-state normal-mode coordinates with a common scaled mass  $m = 1$  a.u.

Keeping  $V_e$  the same in all systems, we construct three different ground-state surfaces  $V_g$  to demonstrate the effects of mode displacement, distortion, and Duschinsky rotation in a cumulative fashion. In each case, a Gaussian wavepacket, which generates the emission spectrum from the ground vibrational level  $|K = \mathbf{0}\rangle$  of  $V_e$ , is propagated for 40000 a.u. (20000 steps with a time step of 2 a.u.) on the surface  $V_g$ .

For each system, we provide examples of emissions from the ground vibrational level, a singly excited level, a level with higher excitations in one mode, and two levels with multi-mode excitations. Specifically, we simulate SVL spectra from initial vibrational levels  $1^a 2^b$ ,  $(a, b) \in \{(0, 0), (1, 0), (0, 3), (1, 1), (2, 1)\}$ , where  $a, b$  denote the vibrational quantum numbers in modes 1 and 2

of the excited electronic state.

The autocorrelation function of the Hagedorn wavepacket associated with each initial vibrational level is computed every two steps using the overlap expressions derived in Ref. 67. The SVL emission spectra are then evaluated by Fourier transforming the autocorrelation functions multiplied with a Gaussian damping function, which results in a spectral broadening with a half-width at half-maximum of  $50 \text{ cm}^{-1}$ . Each spectrum is shifted so that the transition to the vibrational ground level ( $1_0^a 2_0^b$ , where the subscripts denote the final vibrational quantum numbers in the ground electronic state after the transition) is at  $0 \text{ cm}^{-1}$ .

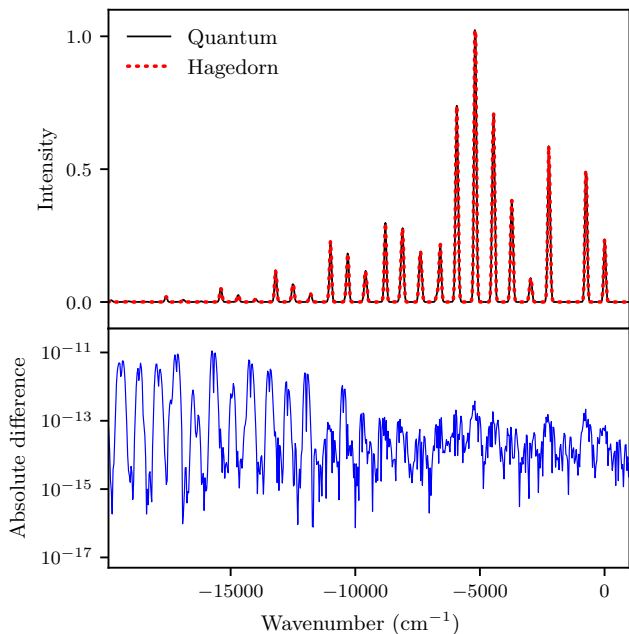


FIG. 1. Comparison of the  $1^2 2^1$  SVL spectra computed using quantum split-operator calculations (black line) and Hagedorn wavepacket dynamics (red dots) in a displaced, distorted, and Duschinsky-rotated two-dimensional harmonic system, with the absolute difference between the two simulated spectra shown in blue in the bottom panel.

To validate the Hagedorn approach, we also propagated the initial states using the second-order Fourier split-operator algorithm on a position grid ranging from  $-128$  to  $128$  in each dimension, with a total of  $256 \times 256$  equidistant grid points. Figure 1 shows the comparison between the exact quantum and the Hagedorn dynamics results in the most complicated case treated here, i.e., the SVL spectrum involving a higher mixed initial excitation ( $1^2 2^1$ ) in the displaced, distorted, and Duschinsky-rotated harmonic model system. This represents the most comprehensive description — within the harmonic oscillator model — of a molecular potential energy surface, which, in reality, has anharmonicity that the global harmonic dynamics considered in this work is not taking into account. The spectrum simulated from Hagedorn

dynamics is not only visually indistinguishable from the grid-based quantum calculation but the absolute differences are also extremely small (on the scale of  $< 10^{-11}$ ). The excellent agreement between the Hagedorn and exact quantum results is also observed in the other simulated SVL spectra, which we now discuss in detail.

Figure 2 contains the SVL emission spectra of the three systems computed using Hagedorn wavepackets. The spectral intensities in all spectra are scaled by the highest peak of the  $1^0 2^0$  spectrum in the displaced, distorted, and rotated system because the other two systems can be thought of as simplified approximations of this most general harmonic system.

If the ground- and excited-state surfaces were not displaced, i.e., if they were identical (up to a constant energy gap  $v_0$ ) with the same equilibrium geometry, the resulting spectrum would consist of a single peak at a wavenumber corresponding to the electronic energy gap. Only transitions with  $\Delta v = 0$  ( $1_a^a 2_b^b$ ) would be allowed since the vibrational wavefunctions with different vibrational quantum numbers  $v$  in the two electronic states would be orthogonal to each other. The horizontal displacement between the two electronic surfaces breaks this symmetry and allows for more vibronic transitions.

In the displacement-only system (first column in Fig. 2), the two displaced surfaces  $V_g$  and  $V_e$  have the same diagonal Hessian matrix  $\kappa_g = \kappa_e$  corresponding to vibrational wavenumbers  $\tilde{\nu}_1'' = 1100 \text{ cm}^{-1}$  and  $\tilde{\nu}_2'' = 1800 \text{ cm}^{-1}$ . Without Duschinsky rotation, the vibronic spectrum is the convolution of the spectrum in each vibrational degree of freedom. Consequently, the peaks for transitions  $1_a^a 2_b^b$  appear at  $\alpha\tilde{\nu}_1'' + \beta\tilde{\nu}_2''$ , where  $\alpha, \beta \in \mathbb{N}_0$ .

The intensity pattern of the SVL spectra is significantly influenced by the initial wavepacket. Higher vibrational excitations in the initial state generally result in more transitions to higher vibrational states on the ground electronic surface, whereas the specific initial excitation allows the selective enhancement (or attenuation) of peaks. For example, in the  $1^0 2^3$  spectrum, significant peaks appear in the  $< -8000 \text{ cm}^{-1}$  region, whereas the  $v_1''$  ( $\beta = 0$ ) peaks, e.g.,  $1_1^0 2_0^3$ ,  $1_2^0 2_0^3$ , and  $1_3^0 2_0^3$  (labeled on spectra), are considerably attenuated compared to the  $1^0 2^0$  spectrum (e.g., peaks  $1_1^0 2_0^0$ ,  $1_2^0 2_0^0$ , and  $1_3^0 2_0^0$ ). The sensitivity of SVL spectra to the initial excitation provides a valuable tool for understanding the vibronic structure in complex molecular systems.

If the ground and excited electronic surfaces no longer have the same vibrational frequencies, the so-called “mode distortion” leads to changes in peak positions as well as in intensity (second column in Fig. 2) in addition to the effects from displacement. In the displaced and distorted system, the initial wavepackets are kept the same, but the force-constant matrix  $\kappa_{g,\text{distorted}}$  defining the ground-state potential  $V_g$  now yields vibrational wavenumbers  $\tilde{\nu}_1'' = 750 \text{ cm}^{-1}$  and  $\tilde{\nu}_2'' = 2200 \text{ cm}^{-1}$ , different from those of the excited-state potential  $V_e$ . We still assume that the normal modes of the two electronic surfaces are aligned, and thus the matrix  $\kappa_{g,\text{distorted}}$  remains

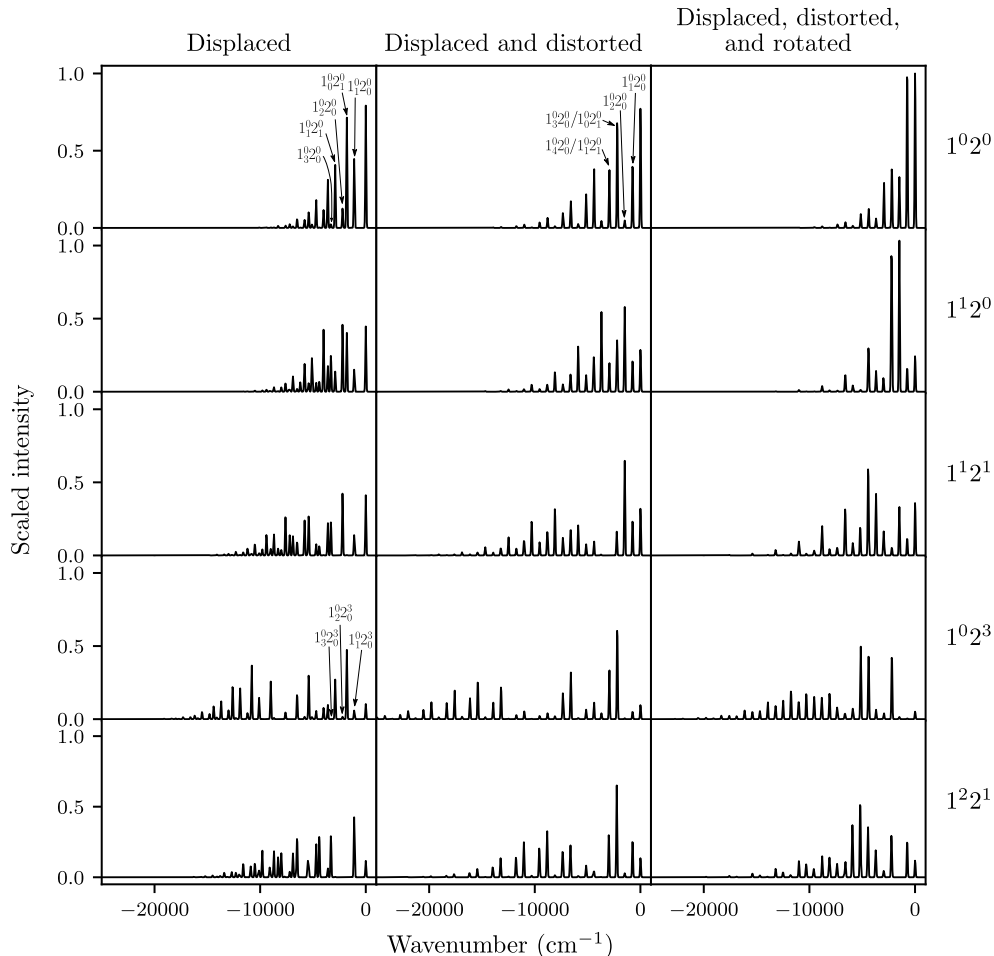


FIG. 2. Simulated SVL emission spectra of three two-dimensional two-state harmonic systems from five different initial vibrational levels (indicated by the labels on the right).

diagonal. As the ground surface changes, the possible peak positions adapt accordingly to the combination of new frequencies, which can be observed by comparing the ordering and positions of the labeled peaks in the  $1^0 2^0$  spectra in the first and second columns. In this particular case, since  $\tilde{\nu}_2'' \approx 3\tilde{\nu}_1''$ , the spectral peaks exhibit a more regular spacing, and certain broadened peaks, e.g. for  $1^0_3 2^0_0$  and  $1^0_2 2^0_1$  (labeled together on the  $1^0 2^0$  spectrum), actually overlap in this displaced and distorted system. The mode distortion also alters the intensity pattern, which is particularly evident in the  $1^1 2^1$  and  $1^2 2^1$  spectra (compare the first and second columns).

Finally, in the Duschinsky-rotated system (third column in Fig. 2),  $V_g$  is modified so that  $\kappa_{g,\text{rotated}} = R(20^\circ)^T \cdot \kappa_{g,\text{distorted}} \cdot R(20^\circ)$ , where

$$R(\theta) = \begin{pmatrix} \cos \theta & -\sin \theta \\ \sin \theta & \cos \theta \end{pmatrix} \quad (18)$$

is a rotation matrix. The analysis of spectra here becomes more challenging, even in two-dimensional systems. Significant differences in the intensity pattern ap-

pear compared to unrotated systems. In our particular case, the frequency range of the spectral region also decreases. From a time-independent perspective, this could be explained by the fact that the Duschinsky rotation reduces the Franck-Condon overlaps between the initial wavepacket and higher vibrational states on the ground electronic surface. Finally, in this most general harmonic model, the propagated Hagedorn wavepackets do not retain the simple, separable form of products of one-dimensional Hermite functions as in Eq. (11), since  $Q_t$  is no longer diagonal when evolved under a Duschinsky-rotated potential. With Hagedorn's ingenious construction, the propagation algorithm maintains its simplicity even for general, non-separable Hagedorn wavepackets, which are not simple products of eigenfunctions of one-dimensional harmonic oscillators.

All spectra shown in Fig. 2 were obtained with the Hagedorn approach and are validated against quantum split operator results in Fig. 3. In contrast to the Hagedorn approach, the quantum dynamics must be performed separately for *each* initial vibrational level in each

system. Where applicable, the Hagedorn results are also compared to the spectra evaluated using the TGA<sup>36,38,68</sup> (for  $1^0 2^0$ ) and its extended version<sup>22,44</sup> (for  $1^1 2^0$  and  $1^1 2^1$ ). Before calculating the differences, the spectra were all scaled and shifted as in Fig. 2. As expected, we observe excellent agreement between the methods. The comparison with the (extended) TGA results serves as a further validation, as these calculations were performed in Heller’s Gaussian parametrization<sup>36,69</sup> that differs substantially from Hagedorn’s. In addition, ETGA employs a different approach to propagate the linear polynomial prefactor of the Gaussian.

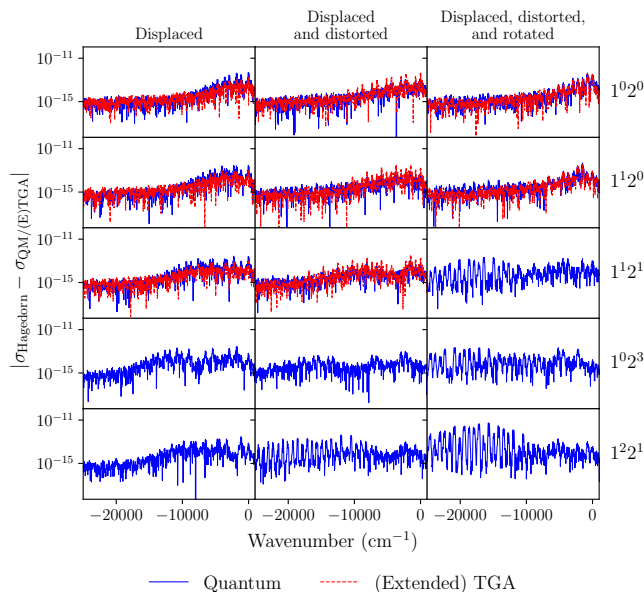


FIG. 3. Absolute differences between scaled spectra computed using Hagedorn wavepackets (Fig. 2) and those obtained with the quantum split-operator algorithm (QM, blue) or (extended) thawed Gaussian approximation [(E)TGA, red].

A notable advantage of Hagedorn wavepackets over the ETGA and the previously reported generating function approach<sup>32</sup> is their ability to simulate dynamics starting from arbitrary initial vibrational levels, going beyond linear polynomial factors. Among the examples shown, the ETGA approach can compute emission from the  $1^1 2^1$  vibrational level only for cases without Duschinsky rotation, where the system can be separated into two one-dimensional systems each with at most a single excitation. The  $1^1 2^1$  spectra were then computed by Fourier transforming the correlation function obtained by multiplying the correlation functions from the two one-dimensional systems.

## B. 100-dimensional displaced, distorted, and Duschinsky-rotated harmonic system

In higher dimensions, the quantum split-operator approach quickly becomes unfeasible due to the curse of dimensionality, particularly when treating excited vibrational wavefunctions for which denser grids are generally needed. In contrast, Hagedorn wavepackets circumvent the need for a grid and can be efficiently propagated within a harmonic approximation using the same trajectory as the guiding thawed Gaussian. With the algebraic expressions from Ref. 67, we can now use Hagedorn wavepackets in much higher dimensions.

Figure 4 shows SVL emission spectra in a 100-dimensional system that incorporates displacement, distortion, and Duschinsky rotation effects (all parameters are specified in the supplementary material). The time step, total time of propagation, frequency of evaluation of the autocorrelation function, and broadening of the spectra are identical to those for the two-dimensional systems. We choose two modes (namely modes 31 and 41) to be vibrationally excited in the initial wavepackets, computing emission spectra from initial vibrational levels  $31^a 41^b$ , with the same set of  $(a, b)$  as in the two-dimensional cases.

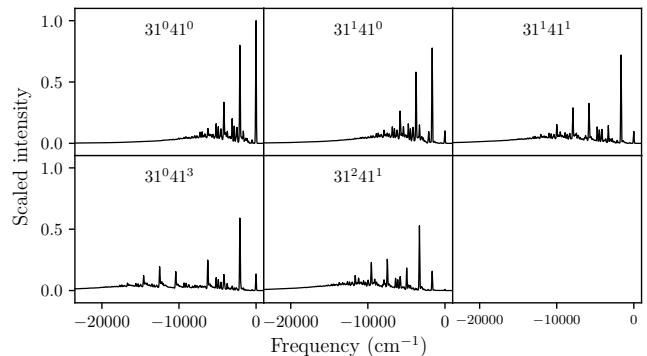


FIG. 4. SVL emission spectra from different vibrational levels (indicated in each panel) in a 100-dimensional two-state displaced, distorted, and Duschinsky-rotated harmonic system.

The spectra become significantly more complex in higher-dimensional systems. In this example, similarity is observed between the  $31^0 41^0$  and  $31^1 41^0$  spectra as well as between the  $31^1 41^1$  and  $31^2 41^1$  spectra. However, significant changes in the intensity pattern appear when comparing spectra with different excitations in mode 41 (compare  $31^0 41^0$  and  $31^0 41^3$ , or  $31^1 41^0$  and  $31^1 41^1$ ), suggesting that the excitation in mode 41 has a more pronounced impact on the overall spectrum compared to the excitation in mode 31. We also observe broadened features in the lower frequency region, which are likely attributable to the effects of Duschinsky rotation here (compare to Fig. S1 where the Duschinsky couplings are neglected).

The initial vibrational excitation in SVL spectra can expand the spectral range and induce transitions to

a large number of highly excited vibrational states of the ground electronic state. Considering, among many other possibilities, only the final vibrational states with five vibrational quanta distributed in three vibrational modes already requires evaluating 970200 transitions (see supplementary material for derivation) at wavenumbers  $> -20000 \text{ cm}^{-1}$ , compared to 10000 evaluations of the autocorrelation function used to generate the spectra in Fig. 4. The actual number of possible transitions is much higher, given the possibility of more quanta distributed among more modes. As a consequence, a sophisticated prescreening is needed. Being a time-dependent approach, Hagedorn wavepacket dynamics can directly capture the broadened feature without the need to compute the huge number of individual transitions that contribute to the tail. In contrast, the time-independent approach can identify contributions from specific transitions, but this is less critical at the relatively low spectral resolution in which we are interested.

The time-independent approach also provides another way to verify our results for the well-resolved  $0 \leftarrow v$  peaks. By computing the Franck-Condon factors for the transition to the ground vibrational level from the different initial states, we confirmed that the changes in the relative intensity of the isolated  $31_0^a 41_0^b$  peaks (at  $0 \text{ cm}^{-1}$ ) in the five spectra with different initial excitations in Fig. 4 are accurately captured (to the fifth decimal place) by the time-dependent Hagedorn approach (see supplementary material).

#### IV. CONCLUSIONS

We have demonstrated that Hagedorn wavepackets offer a robust approach to simulate SVL emission spectra of polyatomic molecules in the harmonic approximation, naturally accounting for mode distortion and Duschinsky rotation effects. Using a single thawed Gaussian trajectory in each system, we were able to evaluate the emission spectra from any vibrational level without incurring additional propagation cost over that required for simulating emission from the ground level. Evaluating the overlaps, the cost of which becomes negligible in *ab initio* applications, represents the only additional step. The excellent agreement between the Hagedorn and grid-based quantum results in two-dimensional examples validates the algebraic expressions we had developed for the overlaps between two general Hagedorn wavepackets.<sup>67</sup> On a 100-dimensional example, we have also demonstrated the feasibility of using Hagedorn wavepackets and our overlap expressions in high-dimensional systems.

In conclusion, Hagedorn wavepackets are well suited for simulating SVL emission spectra. While the present work only considered model potentials, Hagedorn wavepackets can be readily applied to realistic molecular systems using harmonic potentials constructed from *ab initio* electronic structure calculations. Moreover, as in the thawed Gaussian approximation for comput-

ing ground-state emission spectra, anharmonicity effects could be partially captured by propagating Hagedorn wavepackets within local harmonic approximation using on-the-fly *ab initio* data.

Furthermore, the Hagedorn approach presented here could also be adapted to other spectroscopy techniques where the initial state is vibrationally excited or otherwise cannot be adequately described by a single Gaussian wavepacket, such as in the case of vibrationally promoted electronic resonance (VIPER) experiments<sup>34,35,87</sup> or fluorescence-encoded infrared (FEIR) spectroscopy.<sup>88</sup>

#### SUPPLEMENTARY MATERIAL

The supplementary material<sup>89</sup> contains the spectra in the 100-dimensional system without Duschinsky couplings, the parameters of the harmonic systems analyzed in Section IIIB, the comparison with the time-independent approach for the  $0 \text{ cm}^{-1}$  peaks in Fig. 4, as well as the Python program used to compute the overlaps between Hagedorn functions.<sup>67</sup>

#### ACKNOWLEDGMENTS

The authors acknowledge the financial support from the European Research Council (ERC) under the European Union’s Horizon 2020 Research and Innovation Programme (Grant Agreement No. 683069–MOLEQULE).

#### AUTHOR DECLARATIONS

##### Conflict of Interest

The authors have no conflicts to disclose.

#### DATA AVAILABILITY

The data that supports the findings of this study are available within the article and its supplementary material.

<sup>1</sup>R. Marquardt and M. Quack, eds., *Molecular Spectroscopy and Quantum Dynamics* (Elsevier, 2021).

<sup>2</sup>C. S. Parmenter and M. W. Schuyler, *J. Chem. Phys.* **52**, 5366 (1970).

<sup>3</sup>M. Quack and M. Stockburger, *J. Mol. Spectrosc.* **43**, 87 (1972).

<sup>4</sup>T. A. Stephenson, P. L. Radloff, and S. A. Rice, *J. Chem. Phys.* **81**, 1060 (1984).

<sup>5</sup>W. R. Lambert, P. M. Felker, J. A. Syage, and A. H. Zewail, *J. Chem. Phys.* **81**, 2195 (1984).

<sup>6</sup>T. M. Woudenberg, S. K. Kulkarni, and J. E. Kenny, *J. Chem. Phys.* **89**, 2789 (1988).

<sup>7</sup>J. A. Nicholson, W. D. Lawrence, and G. Fischer, *Chem. Phys.* **196**, 327 (1995).

<sup>8</sup>G. Rothschof, T. C. Smith, and D. J. Clouthier, *J. Chem. Phys.* **156**, 184307 (2022).

- <sup>9</sup>F.-T. Chau, J. M. Dyke, E. P.-F. Lee, and D.-C. Wang, *J. Electron Spectrosc. Relat. Phenom.* **97**, 33 (1998).
- <sup>10</sup>F.-T. Chau, J. M. Dyke, E. P. F. Lee, and D. K. W. Mok, *J. Chem. Phys.* **115**, 5816 (2001).
- <sup>11</sup>R. Griminger, D. J. Clouthier, R. Tarroni, Z. Wang, and T. J. Sears, *J. Chem. Phys.* **139**, 174306 (2013).
- <sup>12</sup>D. K. W. Mok, E. P. F. Lee, F.-T. Chau, and J. M. Dyke, *J. Chem. Phys.* **140**, 194311 (2014).
- <sup>13</sup>D. K. W. Mok, E. P. F. Lee, and J. M. Dyke, *J. Chem. Phys.* **144**, 184303 (2016).
- <sup>14</sup>R. Tarroni and D. J. Clouthier, *J. Chem. Phys.* **153**, 014301 (2020).
- <sup>15</sup>T. C. Smith, M. Gharaibeh, and D. J. Clouthier, *J. Chem. Phys.* **157**, 204306 (2022).
- <sup>16</sup>S. Mukamel, *Ann. Rev. Phys. Chem.* **51**, 691 (2000).
- <sup>17</sup>A. Schubert and V. Engel, *J. Chem. Phys.* **134**, 104304 (2011).
- <sup>18</sup>T. Begušić and J. Vaníček, *J. Chem. Phys.* **153**, 184110 (2020).
- <sup>19</sup>T. Begušić and J. Vaníček, *J. Phys. Chem. Lett.* **12**, 2997 (2021).
- <sup>20</sup>M. F. Gelin, L. Chen, and W. Domcke, *Chem. Rev.* **122**, 17339 (2022).
- <sup>21</sup>A. Baiardi, J. Bloino, and V. Barone, *J. Chem. Theory Comput.* **9**, 4097 (2013).
- <sup>22</sup>A. Patoz, T. Begušić, and J. Vaníček, *J. Phys. Chem. Lett.* **9**, 2367 (2018).
- <sup>23</sup>T. Begušić, A. Patoz, M. Šulc, and J. Vaníček, *Chem. Phys.* **515**, 152 (2018).
- <sup>24</sup>M. Bonfanti, J. Petersen, P. Eisenbrandt, I. Burghardt, and E. Pollak, *J. Chem. Theory Comput.* **14**, 5310 (2018).
- <sup>25</sup>A. Prlj, T. Begušić, Z. T. Zhang, G. C. Fish, M. Wehrle, T. Zimmermann, S. Choi, J. Roulet, J.-E. Moser, and J. Vaníček, *J. Chem. Theory Comput.* **16**, 2617 (2020).
- <sup>26</sup>P. P. Roy, S. Kundu, N. Makri, and G. R. Fleming, *J. Phys. Chem. Lett.* **13**, 7413 (2022).
- <sup>27</sup>R. Borrelli and M. F. Gelin, *J. Chem. Phys.* **145**, 224101 (2016).
- <sup>28</sup>T. Begušić and J. Vaníček, *J. Chem. Phys.* **153**, 024105 (2020).
- <sup>29</sup>T. Begušić and J. Vaníček, *Chimia* **75**, 261 (2021).
- <sup>30</sup>L. Chen, R. Borrelli, D. V. Shalashilin, Y. Zhao, and M. F. Gelin, *J. Chem. Theory Comput.* **17**, 4359 (2021).
- <sup>31</sup>J. Huh and R. Berger, *J. Phys. Conf. Ser.* **380**, 012019 (2012).
- <sup>32</sup>E. Tapavicza, *J. Phys. Chem. Lett.* **10**, 6003 (2019).
- <sup>33</sup>A. Baiardi, J. Bloino, and V. Barone, *J. Chem. Phys.* **141**, 114108 (2014).
- <sup>34</sup>J. Von Cosel, J. Cerezo, D. Kern-Michler, C. Neumann, L. J. G. W. Van Wilderen, J. Bredenbeck, F. Santoro, and I. Burghardt, *J. Chem. Phys.* **147**, 164116 (2017).
- <sup>35</sup>M. Horz, H. M. A. Masood, H. Brunst, J. Cerezo, D. Picconi, H. Vormann, M. S. Niraghatam, L. J. G. W. Van Wilderen, J. Bredenbeck, F. Santoro, and I. Burghardt, *J. Chem. Phys.* **158**, 064201 (2023).
- <sup>36</sup>E. J. Heller, *J. Chem. Phys.* **62**, 1544 (1975).
- <sup>37</sup>F. Grossmann, *J. Chem. Phys.* **125**, 014111 (2006).
- <sup>38</sup>M. Wehrle, M. Šulc, and J. Vaníček, *J. Chem. Phys.* **140**, 244114 (2014).
- <sup>39</sup>M. Wehrle, S. Oberli, and J. Vaníček, *J. Phys. Chem. A* **119**, 5685 (2015).
- <sup>40</sup>T. Begušić, J. Roulet, and J. Vaníček, *J. Chem. Phys.* **149**, 244115 (2018).
- <sup>41</sup>T. Begušić, M. Cordova, and J. Vaníček, *J. Chem. Phys.* **150**, 154117 (2019).
- <sup>42</sup>T. Begušić, E. Tapavicza, and J. Vaníček, *J. Chem. Theory Comput.* **18**, 3065 (2022).
- <sup>43</sup>R. Gherib, I. G. Ryabinkin, and S. N. Genin, “Thawed Gaussian wavepacket dynamics with  $\Delta$ -machine learned potentials,” (2024), arXiv:2405.00193.
- <sup>44</sup>S.-Y. Lee and E. J. Heller, *J. Chem. Phys.* **76**, 3035 (1982).
- <sup>45</sup>M. Wenzel and R. Mitric, *J. Chem. Phys.* **158**, 034105 (2023).
- <sup>46</sup>M. Wenzel and R. Mitric, *J. Chem. Phys.* **159**, 234113 (2023).
- <sup>47</sup>With simultaneous multi-mode excitation, although each polynomial factor is linear in its respective dimension, their tensor product is no longer linear. However, without Duschinsky rotation effects, a system remains fully separable at all times and can be treated as several one-dimensional problems.
- <sup>48</sup>G. A. Hagedorn, *Commun. Math. Phys.* **71**, 77 (1980).
- <sup>49</sup>G. A. Hagedorn, *Ann. Phys. (NY)* **135**, 58 (1981).
- <sup>50</sup>G. A. Hagedorn, *Ann. Henri Poincaré* **42**, 363 (1985).
- <sup>51</sup>G. A. Hagedorn, *Ann. Phys. (NY)* **269**, 77 (1998).
- <sup>52</sup>C. Lubich, *From Quantum to Classical Molecular Dynamics: Reduced Models and Numerical Analysis* (European Mathematical Society, Zürich, 2008).
- <sup>53</sup>C. Lasser and C. Lubich, *Acta Numerica* **29**, 229 (2020).
- <sup>54</sup>E. Faou, V. Gradinaru, and C. Lubich, *SIAM J. Sci. Comp.* **31**, 3027 (2009).
- <sup>55</sup>C. Lasser and S. Troppmann, *J. Fourier Anal. Appl.* **20**, 679 (2014).
- <sup>56</sup>H. Dietert, J. Keller, and S. Troppmann, *J. Math. Anal. Appl.* **450**, 1317 (2017).
- <sup>57</sup>T. Ohsawa, *Nonlinearity* **31**, 1807 (2018).
- <sup>58</sup>A. Kargol, *Annales de l’I.H.P. Physique théorique* **71**, 339 (1999).
- <sup>59</sup>G. Hagedorn and A. Joye, *Ann. Henri Poincaré* **1**, 837 (2000).
- <sup>60</sup>V. Gradinaru, G. A. Hagedorn, and A. Joye, *J. Phys. Math. Theor.* **43**, 474026 (2010).
- <sup>61</sup>V. Gradinaru, G. A. Hagedorn, and A. Joye, *J. Chem. Phys.* **132**, 184108 (2010).
- <sup>62</sup>R. Bourquin, V. Gradinaru, and G. A. Hagedorn, *J. Math. Chem.* **50**, 602 (2012).
- <sup>63</sup>E. Kieri, S. Holmgren, and H. O. Karlsson, *J. Chem. Phys.* **137**, 044111 (2012).
- <sup>64</sup>Z. Zhou, *J. Comput. Phys.* **272**, 386 (2014).
- <sup>65</sup>V. Gradinaru and O. Rietmann, *J. Comput. Phys.* **445**, 110581 (2021).
- <sup>66</sup>V. Gradinaru and O. Rietmann, *J. Comput. Phys.* **509**, 113029 (2024).
- <sup>67</sup>J. J. L. Vaníček and Z. T. Zhang, “On Hagedorn wavepackets associated with different Gaussians,” (2024), arXiv:2405.07880.
- <sup>68</sup>E. J. Heller, *Acc. Chem. Res.* **14**, 368 (1981).
- <sup>69</sup>J. J. L. Vaníček, *J. Chem. Phys.* **159**, 014114 (2023).
- <sup>70</sup>E. J. Heller, *J. Chem. Phys.* **75**, 2923 (1981).
- <sup>71</sup>G. A. Hagedorn, *Ann. Phys. (NY)* **362**, 603 (2015).
- <sup>72</sup>T. Ohsawa, *J. Fourier Anal. Appl.* **25**, 1513 (2019).
- <sup>73</sup>M. Combes, *J. Math. Phys.* **33**, 3870 (1992).
- <sup>74</sup>M. Werther, S. L. Choudhury, and F. Großmann, *Int. Rev. Phys. Chem.* **40**, 81 (2020).
- <sup>75</sup>W. Koch, M. Bonfanti, P. Eisenbrandt, A. Nandi, B. Fu, J. Bowman, D. Tannor, and I. Burghardt, *J. Chem. Phys.* **151**, 064121 (2019).
- <sup>76</sup>R. Conte, G. Botti, and M. Ceotto, *Vib. Spectrosc.* **106**, 103015 (2020).
- <sup>77</sup>D. Barbiero, G. Bertaina, M. Ceotto, and R. Conte, *J. Phys. Chem. A* **127**, 6213 (2023).
- <sup>78</sup>M. Thoss, W. H. Miller, and G. Stock, *J. Chem. Phys.* **112**, 10282 (2000).
- <sup>79</sup>G. Herzberg, *Molecular Spectra and Molecular Structure: III. Electronic Spectra of Polyatomic Molecules* (D. Van Nostrand, 1966).
- <sup>80</sup>D. J. Tannor and E. J. Heller, *J. Chem. Phys.* **77**, 202 (1982).
- <sup>81</sup>F. Santoro, R. Improta, A. Lami, J. Bloino, and V. Barone, *J. Chem. Phys.* **126**, 084509 (2007).
- <sup>82</sup>F. Santoro, A. Lami, R. Improta, J. Bloino, and V. Barone, *J. Chem. Phys.* **128**, 224311 (2008).
- <sup>83</sup>J. Tatchen and E. Pollak, *J. Chem. Phys.* **128**, 164303 (2008).
- <sup>84</sup>V. Mohanty and E. J. Heller, *Proc. Natl. Acad. Sci. U.S.A.* **116**, 18316 (2019).
- <sup>85</sup>G. Li, Y.-Y. Zhang, Q. Li, C. Wang, Y. Yu, B. Zhang, H.-S. Hu, W. Zhang, D. Dai, G. Wu, D. H. Zhang, J. Li, X. Yang, and L. Jiang, *Nat. Commun.* **11**, 5449 (2020).
- <sup>86</sup>J. Cerezo and F. Santoro, *J. Comput. Chem.* **44**, 626 (2023).
- <sup>87</sup>L. J. G. W. van Wilderen, A. T. Messmer, and J. Bredenbeck, *Angew. Chem. Int. Ed.* **53**, 2667 (2014).
- <sup>88</sup>L. Whaley-Mayda, A. Guha, S. B. Penwell, and A. Tokmakoff, *J. Am. Chem. Soc.* **143**, 3060 (2021).



<sup>89</sup>Z. T. Zhang and J. J. L. Vaníček, “Single vibronic level fluorescence spectra from hagedorn wavepacket dynamics,” Figshare

(2024), DOI:10.60893/figshare.jcp.c.7428667.v1.